Simulation of the Pressure Field Due to a Submerged Oscillating Jet Impacting on a Solid Wall

Ph. F. Genoux[1]
Direction des Recherches Etudes et Techniques, Paris, France

G. L. Chahine
Tracor Hydronautics, Inc., Laurel, Md.

This paper presents some results obtained with the simulation of a submerged oscillating jet impacting on a solid wall. The oscillating jet which organizes into large vortical structures is simulated by the emission of vortex rings at a constant frequency. Outside of the cores of the rings the fluid is assumed to be inviscid and irrotational. The positions of the tori are obtained by combining for each torus its self-induced velocity with the velocity induced by all other rings and ring-images in the wall. The tangential velocities and the pressures in the fluid at the wall are then computed. The high shearing and suction forces found at the wall may explain the enhanced erosivity and cleaning action of oscillating jets.

Introduction

Experimental observations of air jets show the tendency of the turbulent eddies in their shear layer to organize in large structures. Excitation of a jet with periodic acoustic signals produced upstream of the nozzle by transducers or loud speakers shows a remarkable change of the jet structure into discrete ring vortices, when the excitation frequency, f, matches the predominant natural frequencies of the nonexcited jet [1, 2]. This corresponds to a Strouhal number, S_d, close to 0.3 or one of its first integer multiples. (The Strouhal number is defined as $S_d = fd/V$, where V and d are the velocity and the diameter of the jet.) Based on these observations, several attempts have been carried out to model a jet with a discrete distribution of vortex rings. Axially symmetric vortex rings with a viscous core have been investigated and the numerical schemes were able to satisfactorly reproduce experimental measurements or observations [3-5]. For instance, the fluctuating pressure field in the jet vicinity was simulated by Fung et al. [3]. Acton [4] simulated the upstream portion of the jet with a double row of ring vortices which were allowed to interact and move freely downstream of the nozzle exit. The roll up of the vortex sheet into large axisymmetric structures was numerically demonstrated. Artificial excitation of the jet by periodically modulating the strength of the emitted vortices exhibited the same features as obsrved experimentally, namely the existence of an optimal Strouhal number.

Under an effort for the Department of Energy, in order to improve the erosive and cleaning power of submerged water jets in deep drilling technology, the same ideas were applied to cavitating jets [6]. Here, the cavitation appears in the shear layer in randomly oriented vortex filaments in which gas and vapour cavities grow. The studies conducted at Tracor Hydronautics have shown very clearly that a cavitating jet can be organized in well defined bubble ring vortices when excited (Fig. 1). This has augmented the erosive and cleaning power of these jets. Both external excitation with a transducer and self induced oscillations have been considered [6]. In previous work we modelled the growth and collapse of a toroidal bubble in an infinite medium. A dynamic equation was derived and the importance of the various parameters investigated. The characteristic time of the collapse of the toroidal cavity, and its self induced translation velocity were obtained [7, 8].

This paper is one of the first steps towards the understanding of the enhancement of the cleaning effects associated with the excited jets and is mostly concerned with the interaction of an organized jet with a solid wall. Taking advantage of the numerical results obtained in previous studies and of experimental observations one can simplify the problem by neglecting the fine structure of the jet's shear layer and assuming that the major features of the flow field are associated with the large structures. Thus, the excited jet is modelled with large vortex rings emitted from the nozzle orifice at constant time intervals which correspond to the

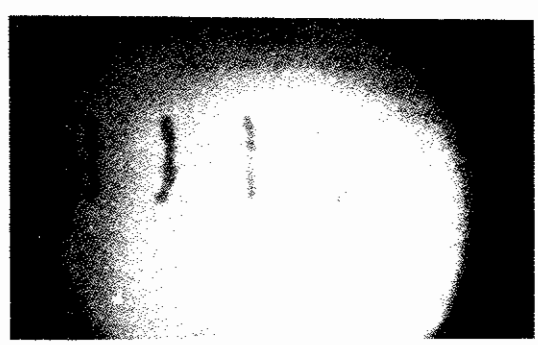

Fig. 1 Cavitating vortex rings in the shear layer of an excited submerged jet. $\sigma = 0.94$, $M = 0.082$, and $F = 14$ kHz

[1] This work was done while on leave at Tracor Hydronautics, Incorporated.

Contributed by the Fluids Engineering Division and presented at the Cavitation and Polyphase Flow Symposium, Houston, Texas, June 20-22, 1983. Manuscript received by the Fluids Engineering Division July 19, 1983.

frequency of the pulsing jet. Each of these vortex rings has in its center a gas and vapor filled toroidal cavity and is allowed to move and change shape under the influence of its self induced velocity as well as the velocities induced by the other ring vortices present in the field. The presence of the wall is accounted for by applying the method of images since no viscous effects are considered. Knowing the location and characteristics of all rings at any time allows the computation of the generated pressure field. We present here the model used and some results on the interactions of the large structures between each other and with the wall, as well as the generated pressures on several arbitrary locations on the solid wall.

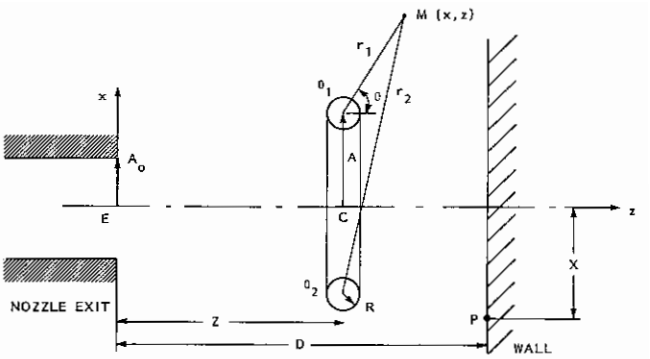

Fig. 2 Definition diagram of the geometry

Formulation of the Problem

Let us consider a vortex ring of radius A_0 and of circulation, Γ, constant in time. The core of the ring is gas and vapor filled and has a circular section of radius R_0. The surface tension coefficient at the bubble liquid interface is γ, and the initial partial gas and vapor pressures inside the bubble are P_{g0} and P_v. Outside the gaseous core we can assume that the liquid is inviscid and incompressible and that the flow is irrotational. Therefore the liquid flow is potential. In order to simplify the analytical and numerical approach we consider the case where the radius of the gaseous section is small compared to the torus radius and introduce the small parameter,

$$\epsilon = R_0/A_0 << 1 \tag{1}$$

We can then consider an asymptotic approach to the problem, and use the method of matched asymptotic expansions. Concerning the investigation of the bubble ring behavior two regions of the fluid field are introduced. In the "inner region" of characteristics length R_0, the problem is concerned with the torus core, and is two-dimensional, and the bubble appears as cylindrical. In the "outer region" of characteristic length A_0, the cavity cannot be distinguished and the problem reduces to the well-known potential problem of a circular vortex line. For this "outer problem" the expression of the stream function ψ is given by Lamb [9].

$$\psi = -\frac{\Gamma}{2\pi}(r_1+r_2)\left[K\left(\frac{r_2-r_1}{r_2+r_1}\right)-E\left(\frac{r_2-r_1}{r_2+r_1}\right)\right] \tag{2}$$

where E and K are complete elliptic integrals of the first and second kind respectively and where the geometric distances r_1 and r_2 are defined in Fig. 2. Similarly, the velocity potential can be written as

$$\phi^{ext} = \frac{-\Gamma}{4\pi}\int_S \frac{\mathbf{PM}\cdot e_z}{|\mathbf{PM}|^3}\,ds$$

$$= \mathrm{sgn}(Z-z)\frac{\Gamma A_0}{2}\int_0^\infty e^{-k|z-Z|}J_0(kx)J_1(kA_0)dk \tag{3}$$

where J_0 and J_1 are the Bessel functions of order 0 and 1, and P is a point of any surface S limited by the circle of radius A_0.

In order to determine the self-induced translation velocity of the vortex ring one has to solve both the inner and outer problems using a matching condition at the boundary of the two regions. For instance, when no bubble growth occurs the behavior of the outer solution in the vicinity of the bubble wall can be obtained by expanding ϕ^{ext} in powers of ϵ and Log ϵ, [8], and can be written:

$$\lim_{\epsilon\to 0}\ \phi^{ext}(\epsilon A_0\tilde{r},\theta)$$

$$= \frac{\Gamma}{2\pi}\left[\theta-\epsilon\mathrm{Ln}\left(\frac{\epsilon}{8}\right)\frac{\tilde{r}}{2}\cos\theta-\epsilon\frac{\tilde{r}\cos\theta}{2}\mathrm{Ln}\,\tilde{r}+\sigma(\epsilon)\right], \tag{4}$$

where the nondimensional distance, $\tilde{r}$, from the bubble center to the field point M is defined by:

$$\tilde{r} = r/R_0 = r/\epsilon A_0 \tag{5}$$

Expression (4) is used for writing the boundary conditions at

Nomenclature

d = jet diameter
e_z = unit vector along z-axis
E = complete elliptical integral of the second kind
f = frequency
Jo = Bessel function of order 0
J_1 = Bessel function of order 1
K = complete elliptical integral of the first kind
$\mathbf{n}$ = normal unit vector
P_{g0} = initial partial gas pressure inside the ring
P_v = vapor pressure inside the ring
P_∞ = pressure at infinity
R = vortex ring section radius
R_0 = initial ring section radius
$r_{1,2}$ = geometric distance between the field point and the ring center
A = vortex ring radius
A_0 = initial vortex ring radius
S = vortex ring surface
S_d = Strouhal number $= fd/V$
t = time
V = jet velocity
Z = axial distance of the ring center
z = axial distance of the field point
$\mathcal{W}_s^{-1}$ = inverse of the Weber number $= \gamma/R_0P_\infty$
X = radial distance from the ring axis
ϵ = asymptotic parameter, defined as the ratio of the ring section radius to the ring radius
γ = surface tension
Γ = circulation of the vortex ring
ψ = stream function
ϕ = velocity potential
θ = field angle
∇ = gradient operator
Δ = Laplacian operator
ρ = density of the liquid
δ = ratio between the core size and the ring radius
Ω_s = circulation parameter $= \frac{\rho}{P_\infty}\left(\frac{\Gamma}{2\pi R_0}\right)^2$

Superscripts

ext = outer problem
int = inner problem
~ = tilde, normalization in reference to the outer problem
— = bar, normalization in reference to the inner problem

infinity for the inner problem, and contains most of the information needed to compute the bubble translation velocity. Besides the vortical motion which is given by the first order term, a uniform velocity appears to the following order, $\epsilon \mathrm{Ln}\,(\epsilon/8)$. More complicated terms appear at the higher orders. If the bubble ring is not isolated the second term is modified by an additional constant multiplying $\bar{r}\cos\theta$.

In the "inner problem", one has to solve the Laplace equation along with kinematic and dynamic boundary conditions on the bubble wall:

$$\Delta\phi^{\mathrm{int}} = 0, \tag{6}$$

$$\nabla\phi^{\mathrm{int}} \cdot \mathbf{n}\Big|_{r=R} = \mathbf{V}_t \cdot \mathbf{n}, \tag{7}$$

$$\rho\left[\frac{\partial\phi^{\mathrm{int}}}{\partial t} - \mathbf{V}_t \cdot \nabla\phi^{\mathrm{int}} + \frac{1}{2}\,|\nabla\phi^{\mathrm{int}}|^2\right]_{r=R} = p_\infty - p_v - p_g - 2\gamma\mathcal{C}, \tag{8}$$

where $\mathbf{n}$ is the normal vector to the bubble wall, $\mathcal{C}$ the bubble curvature, and $\mathbf{V}_t$ the translation velocity of the ring which is chosen as the translation velocity of the origin of coordinates. Equations (6) to (8) are expanded in powers of ϵ and $\mathrm{Log}\epsilon$, and ϕ^{int} and $R(\theta, t)$ decomposed in spherical harmonics. One finds, [8], after using the boundary condition at infinity derived from (4) that the circular shape of the bubble section is a stable solution, up to the order ϵ, and that the self-induced velocity of the ring is

$$V_{\mathrm{self}} = \frac{\Gamma}{4\pi R_0}\left\{\frac{\epsilon}{\bar{A}}\left[\mathrm{Ln}\frac{8\bar{A}}{\epsilon} - \frac{1}{2} + \frac{\mathcal{W}_s^{-1}}{\Omega_s}\right] + 0(\epsilon)\right\}, \tag{9}$$

where $\mathcal{W}_s^{-1}$ is the inverse of the Weber number and Ω_s the circulation number measuring respectively the relative importance of the surface tension and the pressure drop due to circulation relative to the ambient pressure. These are written as:

$$\mathcal{W}_s^{-1} = \gamma/R_0 P_\infty, \tag{10}$$

$$\Omega_s = \rho(\Gamma/2\pi R_0)^2/P_\infty. \tag{11}$$

A similar expression has been obtained for vortex rings with a viscous liquid core. In that case ϵ is replaced by δ, the ratio between the core size and the torus radius, A, the surface tension term is null and the constant 1/2 is replaced by 1/4 [10]

$$V_{\mathrm{viscous}} = \frac{\Gamma}{4\pi R_0}\left\{\delta\left[\mathrm{Ln}\,\frac{8}{\delta} - \frac{1}{4}\right] + 0(\delta)\right\} \tag{12}$$

Numerical Procedure and Remarks

In order to simulate the behavior of the jet and its interaction with the wall we used the following procedure. At $t = 0$, a ring is emitted from the location $Z = 0$ and is allowed to move under the influence of its self-induced velocity. The velocity due to the ring image is to be added when a solid wall is present. Subsequently at the discrete instants $t_n = n/f$, (f is the jet oscillation frequency and n an integer number) an additional ring is emitted and is allowed to interact with the rings already in field and their images. At every time step the locations of all the rings are computed, as well as their translation velocities which in turn determine their subsequent positions. The self-induced velocity of any ring is computed using equation (9), while its translation velocity due to the other rings and the ring images is derived using equations (4) or (5) since the analysis show that the translation velocity of the bubble ring due to an imposed incoming flow is equal to the fluid velocity at its location.

As expected the behavior of the emitted rings is at first unsteady and does not represent the jet behavior. However, after certain computation time has elapsed the system becomes steady and a periodic behavior of the various emitted ring is exhibited. Once the location of all the rings are determined, the pressure at any location can be obtained using the Bernoulli equation:

$$p(M) - p_\infty = -\rho\left[\frac{\partial\phi^{\mathrm{ext}}}{\partial t} + \frac{1}{2}\,|\nabla\phi^{\mathrm{ext}}|^2\right] \tag{13}$$

where ϕ^{ext} is given using (3).

Let us note that in the procedure and the analytical expressions presented above we have neglected both the influence of the nozzle and the bubble growth. The first effect is too complicated to account for with accuracy at the present time and will constitute a future subject of investigation. The bubble growth effect which we have studied earlier [7] can be neglected if the variation of the local pressure around the bubble ring and the influence on the vortex ring motion are small compared to ϵ, the highest order term considered in the above expressions. This is true as long as the distance between two tori is of higher order of magnitude than ϵ, (i.e., as long as the distance is greater than the section radius). This assumption, as we will see below is valid in all the cases studied and fails only when the vortex ring becomes very close to the wall. In fact, in that case not all assumptions are valid and viscous effects on the wall must be considered.

Results and Discussion

In all results presented below, distances are normalized with the nozzle radius, $A_0 = d/2$, and velocities with the self-induced velocity of an isolated ring, V_{selfo}, from (9). Thus the time scale is A_0/V_{selfo}. For comparison purposes, Fig. 3 shows the behavior of the simulated jet in absence of a solid wall. In this case a steady periodic solution appears after about seventeen time steps. Then the multiple rings exhibit similar behavior to two equal rings, namely successive threading and overpassing of one ring through the other. Here all rings emitted at an odd number normalized time follow the same path while all even numbered ones follow a different path. At a given subsequent time the rings are located as those numbered in the figure. The arrowed lines in the figure join two successive rings and show that the closest to each other these rings get is at the moment they pass each other and that even then they stay at a distance of order unity. Figures 4 and

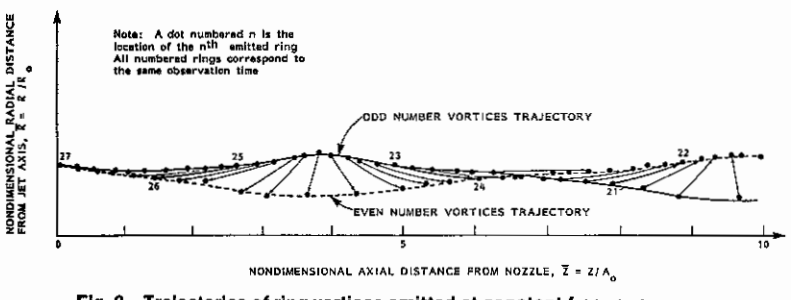

Fig. 3 Trajectories of ring vortices emitted at constant frequency, $\epsilon = 0.1$, $W_e = 200$, $\Omega = 20$, $f = 1$

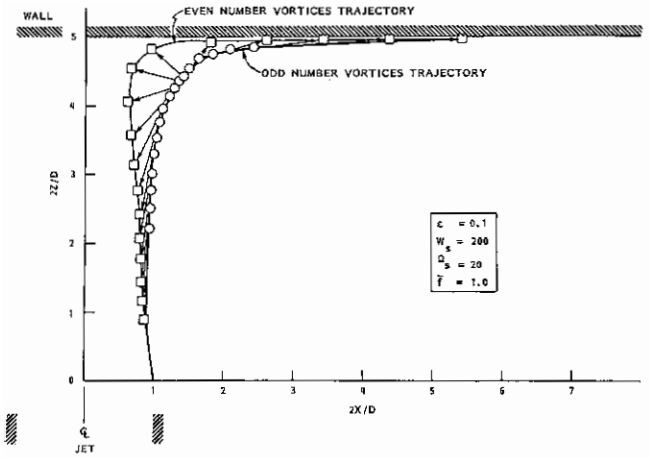

Fig. 4 Trajectories of ring vortices emitted at constant frequency ($S_d = 2f = fd/V\,self_0 = 2$)

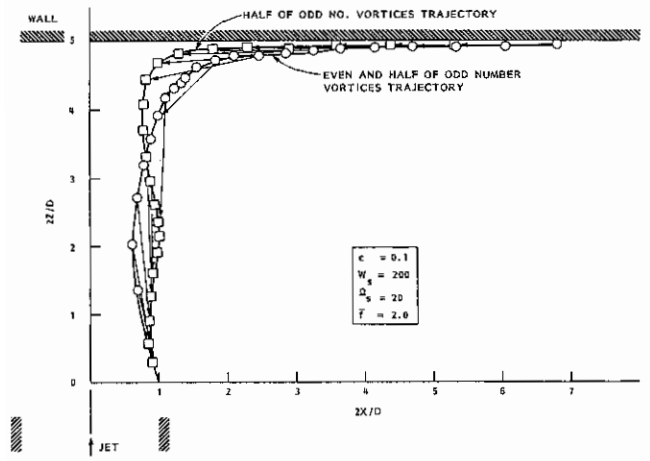

Fig. 5 Trajectories of ring vortices emitted at constant frequency ($S_d = 2f = fd/V\,self_0 = 4$)

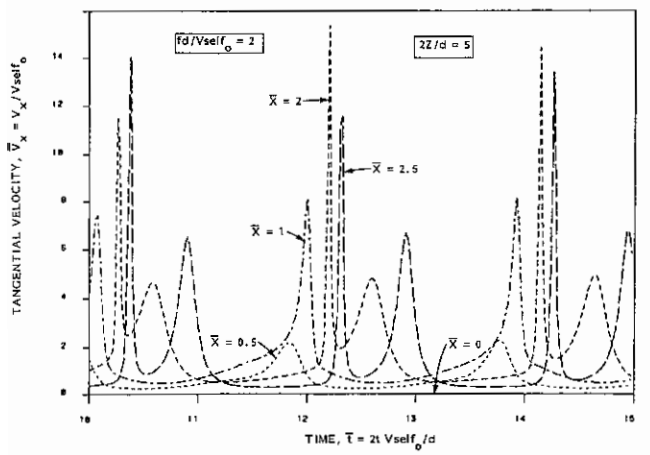

Fig. 6 Tangential velocities induced at different locations, $\bar{X}$, on the impacted wall versus time

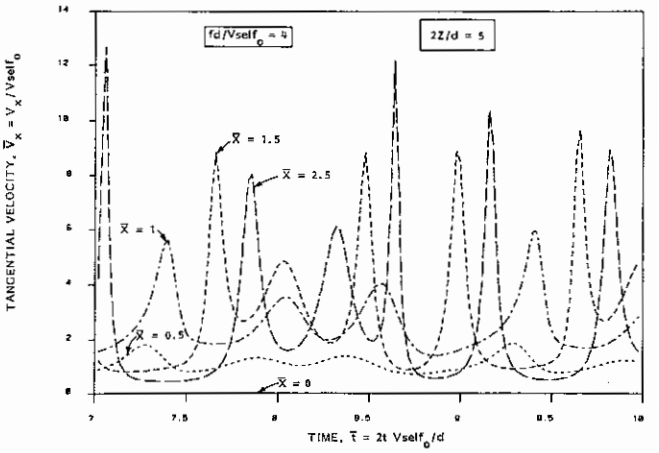

Fig. 7 Tangential velocities induced at different locations, $\bar{X}$, on the impacted wall versus time

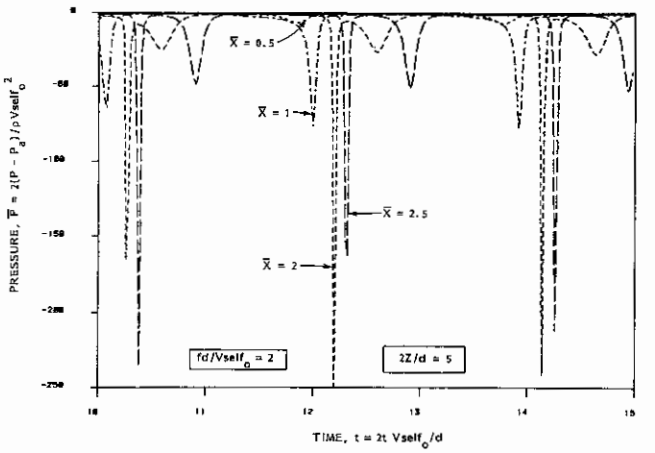

Fig. 8 Pressures induced at different locations, $\bar{X}$, on the impacted wall, versus time

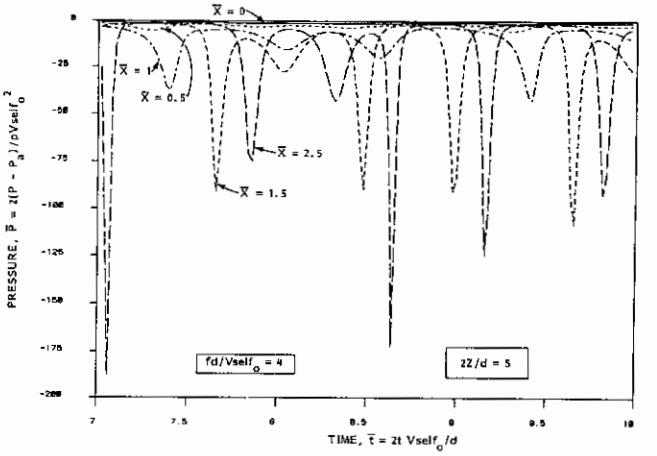

Fig. 9 Pressures induced at different locations, $\bar{X}$, on the impacted wall, versus time

5 show the same type of trajectories represented in-presence of a solid wall and for two reduced frequencies, $\bar{f} = 1$ and 2 (or $\bar{S}_d = f\,V_{self_0}/d = 0.5$ and 1). In both cases the standoff distance, $\bar{Z} = Z/A_0$, is equal to 5. The importance of the Strouhal number on the jet behavior is very clear in this example. Obviously the optimum location of the wall for maximum erosion and cleaning power is not the same for both cases. This optimum is for either maximum pressure fluctuations or maximum tangential velocity (shear) at the wall. In Fig. 4, two distincts trajectories for odd and even number rings is seen as in the free jet case. This is not the case for $S_d \sim 1$, Fig. 5, where all even number rings and one out of two odd number rings follow one trajectory while the other half of the odd number rings follow another. In both cases the steady solution was attained much faster than for the free jet, after

about seven time steps. We can notice also that in both cases two successive rings are always much further apart than ϵ. However their distance to the wall becomes of this order at a radial distance to the jet center, $\bar{X}$, of about 2.5.

Figures 6 and 7 show the tangential velocities induced on five different locations on the solid wall versus time. The spikes correspond to the passage of a vortex ring. It is interesting to notice that both the amplitude and the frequencies of the locally sensed velocity spikes are dependent on the point of observation. The same observations can be made concerning the generated pressures represented in Figs. 8 and 9. The occurrence of the pressure and velocity spikes for both frequencies are very much correlated as well as their amplitudes. Both indicate that the predominant term is the steady term $|\nabla\phi|^2$ and that the major factor with our assumptions appears to be the distance at a given time between the ring and the wall. This explains why the highest negative pressure peaks are at an optimum (in the analyzed range) value of $\bar{X}$. Both, the high intensification of the tangential velocities and of the suction pressures on the wall due to the passage of organized structures indicate a significant enhancement of the cleaning capability of water jets through excitation. This is possible through an increased shearing action of the jet on the solid chips on the wall as well as increased lifting forces. These first results of the developed program are being presently refined through accounting for the bubble volume change near the wall and are being extended to obtain relationships between Strouhal numbers, optimum standoff distances and maximum pressure drop on the wall. The same numerical program can be used for noncavitating vortex rings by replacing equation (9) by (12).

Acknowledgments

This work was supported in part by the U.S. Department of Energy, Division of Geothermal Energy, under SANDIA Laboratories Contract No. 13-5129. We would like to thank V. E. Johnson, H. L. Liu, and W. R. Sirian from Tracor Hydronautics, Incorporated for useful discussions and contributions to the presentation.

References

1 Crow, S. C., and Champagne, F. H., "Orderly Structure in Jet Turbulence," *Journal of Fluid Mechanics*, Vol. 48, Part 3, Aug. 1971, pp. 547–591.

2 Kibens, V., "Discrete Noise Spectrum Generated by an Acoustically Excited Jet," Paper 75-0592, *AIAA Fifth Aeroacoustics Conference*, Mar. 12–14, 1979.

3 Fung, Y. T., Liu, C. H., and Gunzburger, M. D., "Simulation of the Pressure Near a Jet Randomly Distributed Vortex Rings," *AIAA, Journal*, 1979, Vol. 17, pp. 553–557.

4 Acton, E., "A Modelling of Large Eddies in an Axisymmetric Jet," *Journal of Fluid Mechanics*, Vol. 98, 1980, pp. 1–31.

5 Edwards, A. V. J., Morfey, C. L., and Davies, P. O. A. L., "A Computer Simulation of a Starting-Jet," University of Southampton, *ISVR Technical Report No. 89*, Apr. 1977.

6 Johnson, V. E., Jr., Chahine, G. L., Lindenmuth, W. T., Conn, A. F., Frederick, G. S., and Giacchino, G. J., Jr., "Cavitating and Structured Jets for Mechanical Bits to Increase Drilling Rate," ASME Paper 82-P35-13, 1982.

7 Chahine, G. L., and Genoux, Ph., "Collapse of a Vortex Ring," *ASME Cavitation and Polyphase Flow Forum*, Saint Louis, Missouri, June 1982, pp. 37–41. Journal of Fluids Engineering, Vol 105, pp. 400–405, Dec. 1983.

8 Genoux, Ph., and Chahine, G. L., "Equilibre Statique et Dynamique d'un tore de Vapeur Tourbillonnaire," *Journal de Mecanique théorique et Appliquée*, Vol. 2, No. 5, pp. 829–837, Sept. 1983.

9 Lamb, H., *Hydrodynamics*, Dover Publications, Inc., New York, 1932.

10 Safman, P. G., "The Velocity of Viscous Vortex-Rings," *Stud. Appl. Math.*, Vol. 49, 1970, p. 371–380.